

Novel Backoff Mechanism for Mitigation of Congestion in DSRC Broadcast

Seungmo Kim, *Member, IEEE*, and Byung-Jun Kim

Abstract—Due to the recent re-allocation of the 5.9 GHz band by the US Federal Communications Commission (FCC), it will be inevitable that dedicated short-range communications (DSRC) and cellular vehicle-to-everything (C-V2X), two representative technologies for V2X, have to address coexistence. Especially, the distributed nature of DSRC makes it not trivial to control congestions due to an asynchronous structure, which makes it inefficient to disseminate a controlling signal. To this end, we propose a method to “lighten” a distributed V2X networking. Technically, it is to allocate the backoff counter according to the level of an accident risk to which a vehicle is temporarily exposed. We provide an analysis framework based on a spatiotemporal analysis. The numerical results show the improvement in the successful delivery of basic safety messages (BSMs).

Index Terms—V2X, 5.9 GHz, DSRC, CSMA, Backoff

I. INTRODUCTION

1) *Background on the 5.9 GHz Band:* In 1999, the US Federal Communications Commission (FCC) allocated the 5.9 GHz band for intelligent transportation system (ITS) applications based on dedicated short-range communications (DSRC) and adopted basic technical rules for the DSRC operations [1]. The DSRC is now at the stake of sharing the 5.9 GHz band with other radio technologies (RATs).

The first RAT is Wi-Fi. As suggested by the Congress in September 2015, the FCC, in its latest public notice [2], now seeks to refresh the record of its pending 5.9 GHz rulemaking to provide potential sharing solutions between proposed Unlicensed National Information Infrastructure (U-NII) devices and DSRC operations in the 5.9 GHz band. The current focus of the FCC’s solicitation in [2] is two-fold: (i) prototype of interference-avoiding devices for testing; (ii) test plans to evaluate electromagnetic compatibility of unlicensed devices and DSRC.

More recently, the cellular vehicle-to-everything communications (C-V2X) is seeking to operate in the 5.9 GHz band as well [3]. At present, only DSRC is permitted to operate in the ITS band in US, while the 5G Automotive Association (5GAA) has requested a waiver to the FCC to allow C-V2X operations in the band [3]. The key problem here is that C-V2X and DSRC are not compatible with each other. It means that if some vehicles use DSRC and others use C-V2X, these vehicles will be unable to communicate with each other—a scenario where the true potential of V2X communications cannot be attained.

S. Kim is with Department of Electrical and Computer Engineering, Georgia Southern University in Statesboro, GA, USA (e-mail: seungmokim@georgiasouthern.edu). B. J. Kim is with Department of Statistics at Virginia Tech in Blacksburg, VA, USA (e-mail: bjkim702@vt.edu).

2) *Significance of DSRC:* Nevertheless, DSRC still holds significance as the key technology enabling safety-critical applications [4]. Europe recently mandated DSRC as the sole technology operating in the 5.9 GHz band [5]. Also, in the US, 50 state transport departments request reserving the 5.9 GHz band for transport safety [6]. However, state departments of transportation (DOTs) are experiencing confusion and inefficiency in enhancement/expansion of connected vehicle technologies, due to the FCC’s indecisiveness on “shared use” of the 5.9 GHz band with other wireless systems i.e., Wi-Fi and C-V2X [6]. Also, at the US DOT, Phase I of a three-phase testing plan has been completed, which investigated the DSRCs interoperability with the other wireless systems [7]. However, Phase II has not yet even started, which is supposed to involve basic field tests to assess the efficacy of findings from Phase I [8]. Until these real-world tests are completed, one will not know conclusively to what extent, or whether at all, DSRC and the other technologies can operate together without interference, which has significant influence on the vehicle safety and mobility.

3) *Need for Lightening Load in DSRC:* A key requirement of V2V communication is the reliable delivery of safety messages. However, it has been found that a DSRC network can be congested even in simple traffic scenarios due to the limited bandwidth [9]. In addition, the FCC reduced the bandwidth for DSRC from 75 MHz to 10 MHz under possible coexistence with C-V2X [10]. As has been found from previous studies [11]–[17], it is not a trivial problem to achieve coexistence among dissimilar RATs not being able to coordinate with each other.

Relevant proposals modeled the crash risk and used it in enhancement of multiple access in V2X networks [18][19]. Another method is the enhanced distributed channel access (EDCA). However, the complicated backoff model [20] is not practical in the delay-constrained nature of a V2X safety-critical network. According to a latest study [21], the classical DSRC backoff model based on the distributed coordinated function (DCF) already yielded quite low probabilities of transmission within a beaconing period.

Motivated from the limitations of the currently available methods, this paper proposes a multiple access scheme that can be applied to a decentralized V2X network and can be performed at each vehicle without external support from infrastructure—e.g., roadside units (RSUs). The contributions of this paper are summarized as

- First, it defines a formula of a crash risk indicator (or CRI) as a function of the variance of a vehicle’s speed from the neighboring vehicles.

- Second, this paper proposes a novel backoff allocation mechanism for DSRC, based on the CRI. The mechanism features direct compatibility to the currently operated *distributed* V2X networking standards—e.g., DSRC and C-V2X mode 3—due to its simple applicability, which shall be elaborated in Section IV. The distributed nature is worth being kept because of the potential in a wide variety of applications—e.g., blockchain [22].
- It describes a carrier-sense multiple access (CSMA) using a more precise Markov chain taking into account a *packet expiration*, which is idiosyncratically critical to DSRC unlike other IEEE 802.11-based technologies. In fact, our results show that a DSRC network is more constrained by an expiration rather than a collision over the air. The CSMA has a key benefit: once programmed, the protocol can be executed at each vehicle without any scheduling from the infrastructure.
- In addition to the widely accepted classical metrics for providing easy understanding for audience, we also evaluate the proposed protocol based on inter-reception time (IRT) as a metric that adds further perspectives in analysis.

II. RELATED WORK

A. Markov Chain Model for IEEE 802.11p MAC

Carrier sense multiple access with collision avoidance (CSMA/CA) for the general IEEE 802.11 has been modeled as a two-dimensional Markov chain [23]. However, in DSRC, the contention window size does not get doubled even upon a packet collision, which simplifies the Markov chain structure.

The key difference in our model is that for BSM broadcast in a DSRC system, the probability of decrementing a backoff counter is not 1. Also, a Markov chain has been proposed to model on the broadcast of safety messages in DSRC [24]; yet it does not take into account a packet expiration (EXP) during a backoff process. Further, there was another aspect about which the model did not describe completely accurately. According to the IEEE 802.11p-2010 standard [25], the fundamental access method of the IEEE 802.11 medium access control (MAC) is a distributed coordination function (DCF), which shall be implemented in all stations (STAs). Investigating the CSMA/CA written in IEEE 802.11 MAC [23][26], the probability of transmission at the state of backoff being 0 still requires the probability of $1 - P_b$ for a transmission (where P_b denotes the probability of a slot being busy).

Also, the previous models suggested for analyzing the 802.11p beaconing have paid little attention to the varying number of contending nodes [27] and the restricted channel access of the control channel (CCH), i.e., Channel 178 (5.885-5.895 GHz) [28]. Since the 802.11p MAC protocol is a contention-based scheme, the joint effect of the varying number of contending nodes and the restricted channel access may lead the network to perform quite differently [29].

Given the significance of an EXP in determining the performance of a DSRC system, the models cannot be considered to completely accurately characterize the behavior of a safety message broadcast. In this work, we develop a new mathematic model that integrates those two factors.

B. Performance Metric

Motivated from limitations of classical metrics such as packet delivery rate (PDR) and latency, various other metrics have been proposed in the literature. The *inter-reception time (IRT)* is a superior metric in the sense that it is able to display both successful and failed transmissions at once. A latest work proposed an algorithm that adapts the frequency of BSM broadcast according to the IRT [30]. When IRT becomes to exceed a threshold, the frequency of transmission is decremented. The decrement goes until it reaches the minimum. While this work tackles a significant problem of managing the IRT, which much previous work overlooks while relying only on classical metrics such as PDR and latency, it does not provide enough mathematical and analytical detail on how exactly formulate the IRT. The same limitation is observed from other simulation-based work [31][32][33][34][35] and experiment-based work [36][37].

Besides the aforementioned metrics, some other metrics have also been used to evaluate the performance of congestion control techniques. Examples include the probability of successful reception of beacon message [38], update delay [39] as the elapsed time between two consecutive BSMs successfully received from the same transmitter, a 95% Euclidean cut-off error (in meters) [40], and information dissemination rate (IDR) [41].

C. DSRC Performance Enhancement Scheme

1) *EDCA*: There is body of work enhancing the performance of DSRC based on EDCA [43]. However, we remind that this paper particularly aims to enhance the performance of DSRC broadcast by prioritizing vehicles at high crash risks. We consider that the EDCA is not enough to achieve that purpose. First, increasing the load of real time data traffic will increase the collision in the network. Thus, delay time and packet loss percentage will increase more than the requirements of quality of service (QoS) [44]. Second, EDCA is known to be susceptible to additional load [45], which makes inadequate for a dynamic, distributed V2X network. Third, EDCA has been found not be able to support fairness when STAs in a network require diverse QoS requirements [46]. Fourth, as shall be presented in Section VI, a DSRC network is “contention-constrained” rather than collision-constrained due to the backoff process for CSMA. It yields an inefficiency of a too large CW, which in turn causes a very high probability of EXP. On the other hand, a too small CW can cause a collision, but it is rare in DSRC due to a large number of slots within a beaconing period—i.e., 1500 slots with 100 msec of inter-broadcast interval (IBI) and 66.7 μ sec of a slot time [42]. Considering the significance of safety-critical applications (indeed far more significant than delivering “voice” messages at a higher data rate), a more aggressive approach is needed to guarantee prioritization of vehicles with higher crash risk levels;

2) *Protocol Independent of CW*: Elaborating the last point, our desire is to design a protocol that optimizes a DSRC network regardless of CW. In the current 802.11 MAC mechanism, the CW size is dictated to take discrete values from a

bounded finite set [47]. The limitations of this constraint have been investigated [48], to discover that the limitation on the CW size in the main bottleneck in a dense network. Also, the BEB scheme has been found not to provide adequate level of fairness due to little correlation between a backoff time and a CW [49]. Furthermore, the IEEE 802.11 BEB backoff time calculation adjusts extremely rapidly [50]; the node backs off quickly when a collision is detected and also reduces its backoff time to CW_{min} immediately upon a successful transmission. This produces a large variation in the backoff time; every new packet after a successful delivery starts with CW_{min}, which may be too small for a heavy network load. It can easily lead to a higher level of network congestion. For these reasons, application of the current BEB that heavily relies on adaptation of CW has been found inefficient for distributed networks [51].

3) *Inter-RAT Coexistence in the 5.9 GHz Band*: The coexistence problem among dissimilar RATs in the 5.9 GHz band has been discussed in the literature: (i) between DSRC and Wi-Fi [52] and (ii) between DSRC and Wi-Fi/C-V2X [21].

Modification of CSMA was proposed for relieving bandwidth contention among vehicles within an IEEE 802.11p network [53]. The inter-vehicle distance was selected as the factor representing the risk of a crash. A message prioritization scheme among different classes of vehicles was proposed for military vehicles over commercial ones [18]. The key limitation was a relatively simple model for the stochastic geometry: a single junction of two 6-lane road segments. Such an urban model may lose generality when applied to other scenarios.

In another latest work, a reinforcement learning-based approach was proposed to address the dynamicity of a V2X networking environment [54]. Each vehicle needs to recognize the frequent changes of the surroundings and apply them to its networking behavior, which was formulated as a multi-armed bandit (MAB) problem. The MAB-based reinforcement learning enabled a vehicle, without any assistance from external infrastructure, to (i) learn the environment, (ii) quantify the accident risk, and (iii) adapt its backoff counter according to the risk.

III. SYSTEM MODEL

For formulation of the DSRC broadcast performance, this paper establishes the following key assumptions.

Assumption 1 (Node Distribution as PPP). A *generalized “square” space is assumed instead of an example road segment, for the most generic form of analysis as done in a related literature [22]. The environment represented by the system space \mathbb{R}_{sys}^2 , which is defined on a rectangular coordinate with the width and length of D m. Therein, a DSRC network is defined as a homogeneous Poisson point process (PPP), denoted by Φ_D , with the density of $\lambda (> 0)$. The position of vehicle i is denoted by $\mathbf{x}_i = (x_i, y_i) \in \mathbb{R}_{sys}^2$. Note also that the PPP discussed in this paper is a stationary point process where the density λ remains constant according to different points in \mathbb{R}_{sys}^2 .*

It is important to note that based on the modeling with PPP, the uniformity property of a homogeneous point process can be held [56]. That is, if a homogeneous point process is defined on a real linear space, then it has the characteristic that the positions of these occurrences on the real line are uniformly distributed. Therefore, we can assume that the DSRC vehicles are uniformly randomly scattered on the road with different values of intensities and CW values, which will be provided in Section VI.

Assumption 2 (Four Types of Packet Transmission Result). *There are four possible results of a packet transmission including successful delivery (SUC) and two types of collision: synchronized transmission (SYNC) and hidden-node collision (HN) [55]. A SUC is a case where a packet does not undergo contention nor collision. A SYNC refers to a situation where more than one Tx’s start transmission at the same time. A HN is the other type of collision, which occurs due to a hidden node.*

Assumption 3 (Consideration of BSM Broadcast in CCH). *The analysis framework and result that will be presented throughout this paper are based on assumption of using the CCH only—i.e., channel 178 in the 5.9 GHz band. It means that the result has a room for improvement if the network’s channel selection is expanded among the other shared channels (SCHs). As such, the results that will be demonstrated in Section VI can be regarded as the worst-case, most conservative ones.*

Assumption 4 (Speed as the Representative Factor of Crash Risk). *Speed has been found as the most direct indicator of a crash risk [59]. This paper assumes that each vehicle moves at speed of v meters per second (m/s), which is a varied factor as shall be shown in Section VI. The direction of a vehicle follows a uniform distribution in the range of $[0, 2\pi]$. A node is bounced off when reaching at the end of \mathbb{R}^2 in order to stay in the space, which hence keeps the total intensity the same.*

Remark 1 (Distribution of vehicle speed). *Speeds are selected by the driver. Different drivers select different speeds, dependent upon many variables (vehicle limitations, roadway conditions, driver ability, etc.). No single speed value can accurately represent all the speeds at a certain location. A speed distribution provides that information. Operating speeds have been found to be normally distributed [58]. This is fortunate since using that premise (probability is normally distributed) allows for some straightforward calculations.*

Definition 1 (Variance of speed: crash risk measurement metric). *We use the variance of speed from the speed limit of the road as the metric measuring the risk of a crash. The rationale behind this is the “easiness” in getting a speed limit. For instance, a speed limit is an easy number to obtain in many commercial GPS applications (e.g., Google Maps). Reliance on such an easily available quantity increases the applicability of the proposed algorithm. It can be replaced*

with other relevant parameters: e.g., the mean speed over the neighboring vehicles.

$$\Psi = \sqrt{(v - v_L)^2} \quad (1)$$

where v_L gives the speed limit of the road.

Definition 2 (Marked point process). *The PPP Φ is defined as a “marked” point process where the speed variance, Ψ , is associated with each point \mathbf{x}_i . This mark is an independent normal random variable as seen from a point \mathbf{x}_i . Specifically, let point process $\Phi = \{\mathbf{x}_i; i \in \mathbb{N}\}$ denote the locations of the nodes.*

Importantly, it is assumed that the mark of a point does not depend on the location of its corresponding point in the underlying (state) space.

IV. PROPOSED PROTOCOL

As have already mentioned in Section III, we choose the variation of speed, denoted by Ψ , as the key indicator of a crash risk to a vehicle is exposed while driving. As such, the proposed protocol allocates the backoff counter according to the quantity of Ψ .

We wanted a more aggressive scheme to benefit “dangerous” vehicles than allocating a higher access category (AC) in EDCA. In essence, the performance of EDCA still depends on CW, which may be hazardous for a very urgent safety-related packet delivery.

We remind that the key metric in the proposed protocol is Ψ that was presented in Proposition 1. The main idea of the proposed protocol is to divide the distribution of Ψ into multiple *discrete sections* and apply different *backoff allocation patterns*.

As such, we start with formulating the distribution of Ψ . We find the probability distribution function (PDF) as in the following Lemma:

Lemma 1 (Distribution of Ψ). *As shown in Fig. 1, the speed’s variance, Ψ , is found to follow the following distribution:*

$$f_{\Psi}(\psi) = \frac{1}{\sqrt{2\pi}\sigma} \psi^{-\frac{1}{2}} e^{-\frac{\psi}{2\sigma^2}}, \quad \psi \geq 0 \quad (2)$$

Proof: Let random variable Ψ be defined as $\Psi = (X - \mu)^2$ where $X \sim \mathcal{N}(\mu, \sigma^2)$.

For $\psi < 0$, since Ψ cannot have a negative value,

$$\mathbb{P}(\Psi < \psi) = 0 \quad (3)$$

For $\psi \geq 0$,

$$\begin{aligned} \mathbb{P}(\Psi < \psi) &= \mathbb{P}\left((X - \mu)^2 < \psi\right) \\ &= \mathbb{P}\left(-\sqrt{\psi} < X - \mu < \sqrt{\psi}\right) \\ &= \mathbb{P}\left(-\sqrt{\psi} + \mu < X < \sqrt{\psi} + \mu\right) \\ &= F_X\left(\mu + \sqrt{\psi}\right) - F_X\left(\mu - \sqrt{\psi}\right) \end{aligned} \quad (4)$$

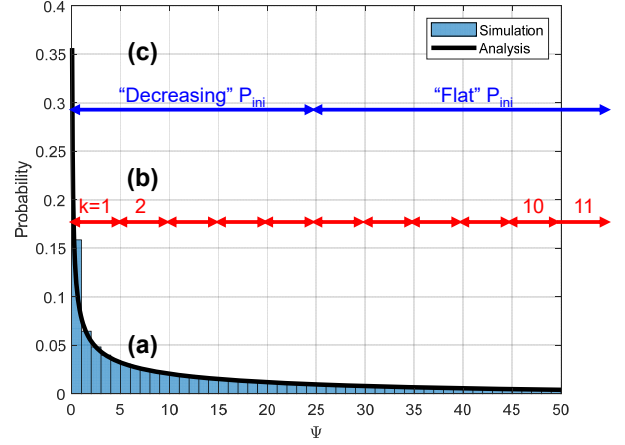


Fig. 1: PDF of Ψ (with $X \sim \mathcal{N}(60, 25)$): (a) Model validation between simulation and analysis of $f_S(s)$; (b) Categorization of Ψ (with $K = 11$ and $Q = 5$); and (c) An example allocation of backoff values for the proposed protocol (division of “decreasing” and “flat” at $k = \lfloor K/2 \rfloor$)

Therefore,

$$\begin{aligned} f_{\Psi}(\psi) &= \frac{d}{d\psi} \left[F_X(\mu + \sqrt{\psi}) - F_X(\mu - \sqrt{\psi}) \right] \\ &= \frac{d}{d\psi} \left[\int_{-\infty}^{\mu + \sqrt{\psi}} \frac{1}{\sqrt{2\pi}\sigma} e^{-\frac{(t-\mu)^2}{2\sigma^2}} dt \right. \\ &\quad \left. - \int_{-\infty}^{\mu - \sqrt{\psi}} \frac{1}{\sqrt{2\pi}\sigma} e^{-\frac{(t-\mu)^2}{2\sigma^2}} dt \right] \\ &= \frac{1}{\sqrt{2\pi}\sigma} \frac{d}{d\psi} \left[\int_{-\infty}^{\mu + \sqrt{\psi}} e^{-\frac{(t-\mu)^2}{2\sigma^2}} dt - \int_{-\infty}^{\mu - \sqrt{\psi}} e^{-\frac{(t-\mu)^2}{2\sigma^2}} dt \right] \\ &= \frac{1}{\sqrt{2\pi}\sigma} \left[e^{-\frac{\psi}{2\sigma^2}} \frac{d}{d\psi} (\mu + \sqrt{\psi}) - e^{-\frac{\psi}{2\sigma^2}} \frac{d}{d\psi} (\mu - \sqrt{\psi}) \right] \\ &= \frac{1}{\sqrt{2\pi}\sigma} \left[e^{-\frac{\psi}{2\sigma^2}} \frac{1}{2} \psi^{-\frac{1}{2}} + e^{-\frac{\psi}{2\sigma^2}} \frac{1}{2} \psi^{-\frac{1}{2}} \right] \\ &= \frac{1}{\sqrt{2\pi}\sigma} \psi^{-\frac{1}{2}} e^{-\frac{\psi}{2\sigma^2}} \end{aligned} \quad (5)$$

which completes the proof. \blacksquare

To represent the crash risk, we categorize the metric, Ψ , into a number of regions on its PDF. The reason for this categorization is, as seen from Fig. 1, the PDF of Ψ is open-ended to the right (positive side); hence, a value of Ψ itself is not appropriate to be used in categorization.

Proposition 1 (Categorization of Ψ). *Note that two key parameters are defined to identify a categorization: (i) the number of categories, K , and (ii) the step size, Q . The range of Ψ for each category, k , is given by*

$$(k-1)Q + 1 \leq \Psi \leq kQ, \quad (6)$$

which, in turn, gives k as a function of Ψ as

$$k = f(\Psi) = \left\lceil \frac{\Psi}{Q}, \frac{(\Psi-1)}{Q} + 1 \right\rceil, \quad k \in \mathbb{Z} \quad (7)$$

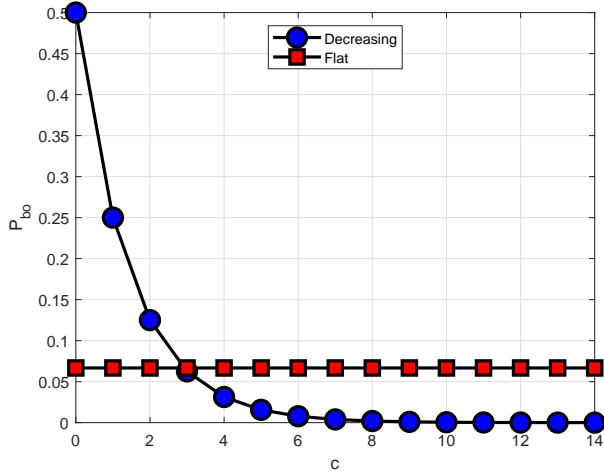


Fig. 2: P_{ini} versus $c \in \{0, 1, \dots, CW - 1\}$ (with $CW = 15$) according to the “decreasing” (proposed) and “flat” (traditional) patterns of backoff counter allocation

Assumption 5 (Fixed k during a backoff allocation process). During a backoff process for a BSM that is shown in Fig. 3, the value of k is assumed to be fixed; in other words, a vehicle does not experience a change of Ψ greater than Q . We assume 10 Hz of the BSM generation frequency—i.e., 10 BSMs per second, which leads to 100 msec per BSM. Notice that a 100 msec is a short time in relation to the reality on the road—i.e., for a vehicle to experience a change in Ψ . Moreover, even if so, as an IEEE 802.11-based system, DSRC is supposed to support such a situation at “best effort.”

We define two types of backoff allocation function versus $c \in \{0, 1, \dots, CW - 1\}$:

Definition 3 (Backoff allocation according to Ψ). *The proposed protocol allocates $P_{bo}(c) := \mathbb{P}[\text{backoff} = c]$ based on the categorization of Ψ into k , as described in Proposition 1 and Fig. 1. The formulation is given by*

$$P_{ini}(c, k) := \mathbb{P}[\text{backoff} = c], \quad \text{where } c \in \{0, 1, \dots, CW - 1\}$$

$$= \begin{cases} r^{c+1} \text{ (“Decreasing”)}, & k > \lceil \frac{K}{2} \rceil \\ \frac{1}{CW} \text{ (“Flat”)}, & k \leq \lfloor \frac{K}{2} \rfloor \end{cases} \quad (8)$$

where term r indicates the intensity of decrease in a $P_{bo}(c)$ and is defined as $r = 1/2$ to make $\sum_{c=0}^{CW-1} P_{ini} = 1$, which is a mathematical requirement to make a Markov chain valid.

More specifically, with a value of k being larger than $\lceil \frac{K}{2} \rceil$ (i.e., the area of “large” Ψ ’s, which indicates cases of greater deviations in a vehicle’s speed), we allocate backoff counters in a “decreasing” pattern. In contrast, for k being smaller than $\lceil \frac{K}{2} \rceil$ (i.e., the area of “small” Ψ ’s, which means cases of smaller deviations in a vehicle’s speed), the backoff counters are allocated in a traditional “flat” fashion in which the probability of any backoff counter value is equal.

Fig. 1 demonstrates an example with $K = 11$ and $Q = 5$. On the PDF, it indicates the principle of the proposed protocol (which shall be described in Section IV): a larger value of $k \in$

$\{1, 2, \dots, K\}$ (which occurs with a smaller probability, $f_S(s)$) takes a smaller backoff value with a higher probability, P_{ini} , as shall be given in (8).

Remark 2 (Interpretation of (8)). *In a “decreasing” backoff allocation, a node is given a higher probability for a smaller backoff value, which increases the chance of winning the medium. A “flat” pattern indicates backoff allocation in a uniform distribution, which is currently adopted by DSRC [21].*

Analyzing Definition 3 further, we can proceed to quantify the probability that a vehicle is allocated a backoff counter following either a decreasing or a flat type function.

Proposition 2 (Probabilities of “decreasing” and “flat” backoff allocation functions). *The proportion of nodes being allocated decreasing and flat patterns of P_{ini} is a predominating factor determining the performance of the proposed system. The proposed protocol determines the proportion by setting a division point in terms of k , to the left and the right of which are assigned for decreasing and flat patterns, respectively. This division can be formally written as*

$$P_{dec} = \int_0^{Q \lceil \frac{K}{2} \rceil} f_{\Psi}(\Psi) d\Psi$$

$$= \int_0^{Q \lceil \frac{K}{2} \rceil} \frac{1}{\sqrt{2\pi}\sigma} \psi^{-\frac{1}{2}} e^{-\frac{\psi}{2\sigma^2}} d\Psi$$

$$= \left[\text{erf} \left(\frac{\sqrt{\Psi}}{\sqrt{2}\sigma} \right) \right]_0^{Q \lceil \frac{K}{2} \rceil}$$

$$= \text{erf} \left(\frac{\sqrt{Q \lceil \frac{K}{2} \rceil}}{\sqrt{2}\sigma} \right) \quad (9)$$

and

$$P_{flat} = \int_{Q \lfloor \frac{K}{2} \rfloor}^{\infty} f_{\Psi}(\Psi) d\Psi$$

$$= \left[\text{erf} \left(\frac{\sqrt{\Psi}}{\sqrt{2}\sigma} \right) \right]_{Q \lfloor \frac{K}{2} \rfloor}^{\infty}$$

$$= 1 - \text{erf} \left(\frac{\sqrt{Q \lfloor \frac{K}{2} \rfloor}}{\sqrt{2}\sigma} \right) \quad (10)$$

where σ denotes the standard deviation of random variable Ψ .

Observing Fig. 1 again, the lefthand and righthand sides of the area under the PDF of Ψ are P_{dec} and P_{flat} , respectively.

It will be worth noticing a few remarks on the proposed protocol, which are given as follows:

Remark 3 (Tx filtering as thinning of Φ). *Such a filtering of Tx vehicles by using the proposed protocol is formulated as a thinning of the PPP Φ . The thinned process has a new intensity, $\tilde{\lambda} \leq \lambda$. The rationale has already been mentioned in Proposition 1. The proposed protocol is expected to grant a higher chance of transmission for vehicles with higher crash risks. As such, when a vehicle’s speed varies too much from*

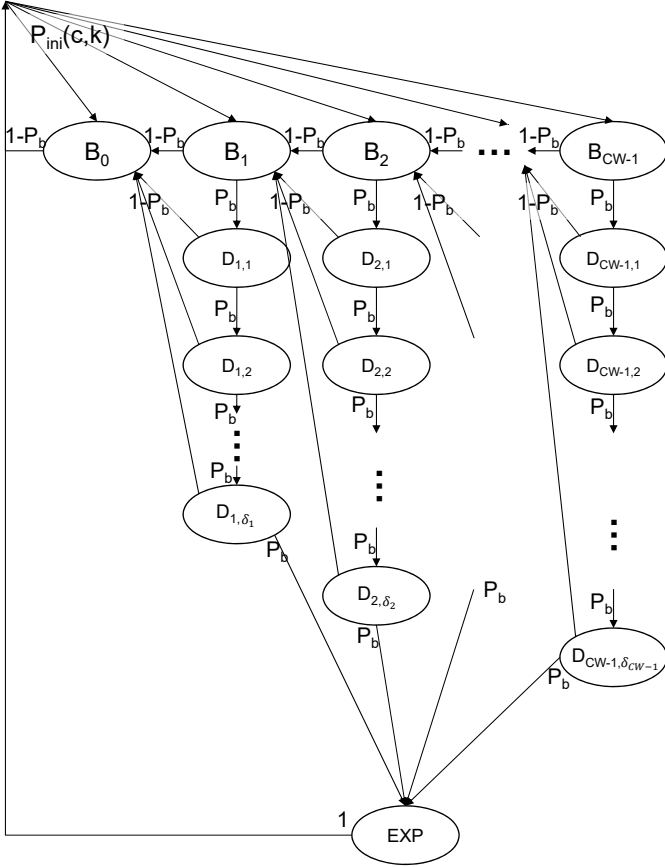


Fig. 3: The proposed protocol as a Markov chain

the speed limit, the vehicle is easily able to broadcast a packet since such a large value of Ψ takes a low probability as shown in Fig. 1.

Remark 4 (Backward compatibility of the proposed protocol). *The key benefit of the proposed protocol is modification of the CSMA that is already adopted in DSRC. As such, it will achieve a higher backward compatibility and therefore an easier adoption in practice.*

V. STOCHASTIC ANALYSIS

For stochastic analysis, the proposed protocol operated at a vehicle is modeled as a one-dimensional Markov chain as illustrated in Fig. 3. We use fixed-point iterations to solve the model.

A. Markov Chain Representation of DSRC CSMA/CA

To recall, in IEEE 802.11 DCF CSMA/CA [26], if no medium activity is indicated for the duration of a particular backoff slot, then the backoff procedure shall decrement its backoff time by a slot time. If the medium is determined to be busy at any time during a backoff slot, then the backoff procedure is suspended; that is, the backoff timer shall not decrement for that slot. The medium shall be determined to be

idle for the duration of a DIFS period or EIFS, as appropriate, before the backoff procedure is allowed to resume.

As shown in Fig. 3, we adopt a key approximation [60]: at each backoff state B_c , due to being asynchronous among the nodes competing for the channel (as referred to from Proposition 3), each packet collides with constant and independent probability of a slot being found busy, P_b .

As another reminder, the key difference between the traditional DSRC and our proposed backoff allocation scheme lies in P_{ini} . The traditional DSRC adopts the CSMA/CA in which the probability of being allocated a backoff counter is uniform among all the B_c 's with $c \in \{0, 1, \dots, CW - 1\}$. In comparison, the proposed scheme differentiates this probability according to the variation of the speed, Ψ . This makes significant difference in the probability of a packet transmission since, depending on the value of P_b , it can be very difficult to make it through the Markov chain and reach B_0 . Specifically, the proposed protocol allocates higher probabilities of starting the chain from B_c 's with smaller c 's to a vehicle with a larger Ψ . Especially when P_b is higher and thus challenging to propagate toward B_0 , the proposed protocol will significantly prioritize the vehicles with large Ψ 's in the medium competition. Furthermore, as have mentioned in Section I, this is the first work to completely precisely display the effect of an EXP.

In the Markov chain shown in Fig. 3, $D_{c,m}$ where $c \in \{0, 1, \dots, CW - 1\}$ and $m \in \{1, 2, \dots, \delta_c\}$ denotes state of the m th delay at backoff state B_c . The deepest state of a delay, D_{c,δ_c} , means the last possible delay for decrement of the backoff counter from c to $c-1$ before expiration of the packet.

B. Probability of Transmission in a Beacon Period

Let τ denote the probability that a node transmits in any slot within a beaconing period (which is composed of L_{bcn} slots). In other words, τ gives the probability that a node has been able to reach B_0 in the Markov chain after going through the backoff process within a beaconing period without experiencing a packet expiration.

One key factor determining a τ is P_b , which denotes the probability that the tagged vehicle observes a slot busy. We remind that P_b is a function of CW and k . (See Remark 2.) That is, in theory, even with a same n_{cs} , different combinations of Ψ can lead to different values of P_b . However, as shall be described in Proposition 3, we have discovered that due to DSRC being an asynchronous system, P_b can be approximated to follow a uniform distribution.

Proposition 3 (Approximation of P_b to uniform distribution). *Although each vehicle is to take different patterns (i.e., {decrease, flat}) depending on its speed variation, Ψ , an overall channel occupancy that is observed as a sum of multiple nodes' transmissions is approximated to follow a uniform distribution. The key rationale behind it is the fact that the transmissions among the competing nodes are "asynchronous," which yields each of the nodes transmits at widely diverse time instants.*

Fig. 4 suggests that such a summation of multiple nodes' transmissions is approximated as a uniform distribution. It is

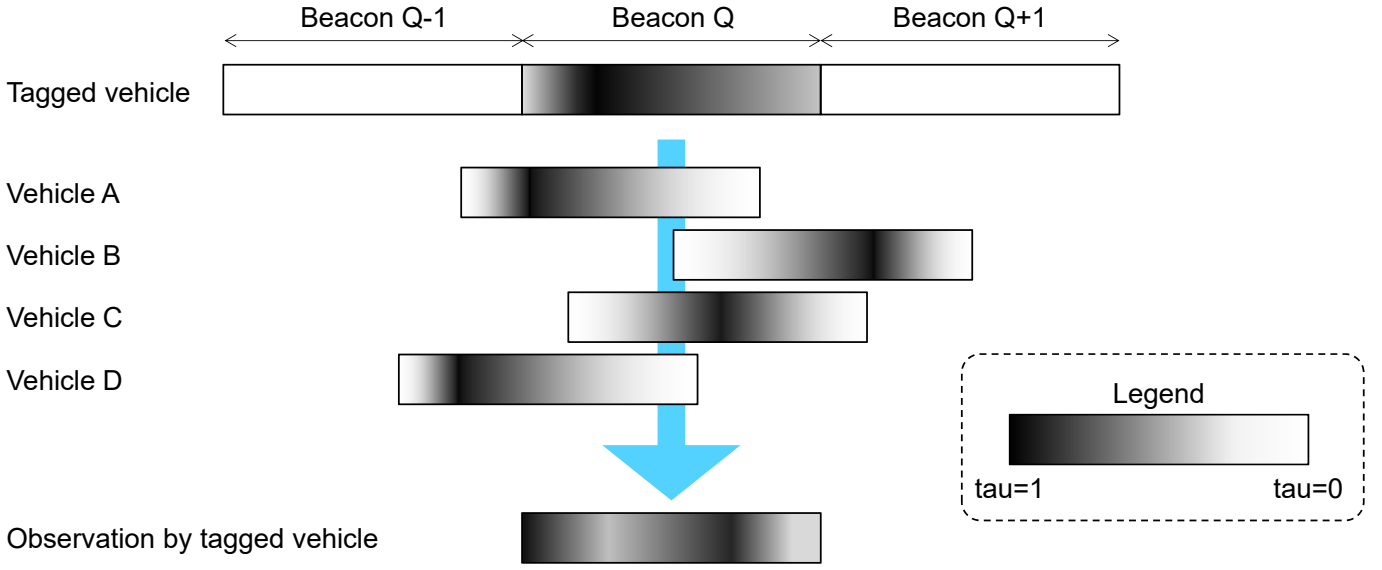


Fig. 4: Approximation of a sum of multiple τ_c 's from multiple nodes to a uniform distribution

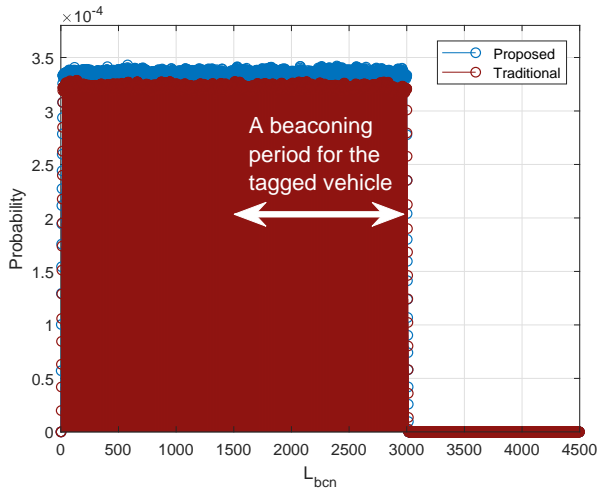


Fig. 5: A snapshot of sum of τ_c 's from n_{cs} nodes (with $n_{cs} = 10$ and $L_{bcn} = 1500$)

intuitive that this approximation will become more accurate as the number of competing vehicles increase.

More specifically, Fig. 5 shows a snapshot of sum of τ_c 's from 10 nodes after 10^6 drops. In addition to a current beaconing period of a tagged vehicle, its previous and next beaconing periods are demonstrated as well. The reason is that other vehicles' beaconing periods are not aligned; hence, their transmissions in the previous and next beaconing periods can also affect the tagged vehicle's current beacon transmission. The other vehicles' occupancy was not considered further than the previous and the current beaconing periods since they do not affect the tagged vehicle's transmission in the current beaconing period.

Fig. 5 also has a suggestion on the comparison between the traditional and proposed CSMA/CA. As observed from the two PMFs, the proposed scheme introduces almost negligible

amount of increase in P_b due to the relatively small number of nodes taking the "decreasing" backoff allocation pattern. We remind that it is exactly what the proposed protocol targeted to achieve: keeping the overall system performance unsacrificed while favoring the dangerous vehicles in a backoff process.

Being uniform, the probability is approximated at $1/3000$; note that the 3000 came from the number of slots in which the other vehicles were able to transmit, i.e., $2L_{bcn} = 3000$. In the proposed protocol, a slightly higher probability of other vehicles' activities is observed since some vehicles were able to complete the backoff process with higher probabilities than in the traditional CSMA/CA. As a consequence, the significance of each time slot among L_{bcn} of them can be approximated as $1/(2L_{bcn})$.

Proposition 4 (Transition matrix of the Markov chain). *The transition matrix for the Markov chain (presented in Fig. 3) is denoted by \mathcal{M} , which is formulated in (11) where $\delta_c \in \mathbb{Z}$ gives the maximum number of busy slots that a node can experience before a packet expiration (EXP) at backoff state c , which is formally written as*

$$\delta_c = \delta_c = L_{bcn} - l_{bcn} - ((CW - 1) - c) \quad (13)$$

with $c \in \{0, 1, \dots, CW - 1\}$. Note that $-l_{bcn}$ comes from the length of a BSM itself, while $-((CW - 1) - c)$ comes from the number of backoffs that has to be decremented.

Proposition 5 (One-step steady-state transition). *Let $P_{B_c} = \lim_{t \rightarrow \infty} \mathbb{P}[B(t) = B_c]$, with $B(t)$ giving a backoff counter state at time t and $c \in \{0, 1, \dots, CW - 1\}$, be the stationary distribution of the chain to obtain the steady-state expressions for the Markov chain. A one-step transition between two arbitrary states (i.e., $B_c \rightarrow B_{c-1}$) in steady state for the Markov chain can be formulated as in (12). Note from (a) that the probability of state B_c is composed of two parts: (i) directly from B_0 and (ii) via B_{c+1} . As shown in (b), the same holds for B_{c+1} , from which one can infer the pattern of*

$$\mathcal{M} = \begin{matrix} & B_0 & B_1 & \cdots & B_{CW-1} & D_{1,1} & \cdots & D_{1,\delta_1} & \cdots & D_{CW-1,1} & \cdots & D_{CW-1,\delta_{CW-1}} & EXP \\ \begin{matrix} B_0 \\ B_1 \\ \vdots \\ B_{CW-1} \\ D_{1,1} \\ \vdots \\ D_{1,\delta_1} \\ \vdots \\ D_{CW-1,\delta_1} \\ EXP \end{matrix} & \left[\begin{array}{cccccccccccc} P_{ini}(0,k) & P_{ini}(1,k) & \cdots & P_{ini}(CW-1,k) & 0 & 0 & 0 & \cdots & 0 & \cdots & 0 & \cdots & 0 \\ 1-P_b & 0 & \cdots & 0 & P_b & \cdots & 0 & \cdots & 0 & \cdots & 0 & \cdots & 0 \\ \vdots & \vdots & \ddots & \vdots & \vdots & \ddots & \vdots & \ddots & \vdots & \ddots & \vdots & \ddots & \vdots \\ 0 & 0 & \cdots & 0 & 0 & \cdots & 0 & \cdots & P_b & \cdots & 0 & \cdots & 0 \\ 1-P_b & 0 & \cdots & 0 & 0 & \cdots & 0 & \cdots & 0 & \cdots & 0 & \cdots & 0 \\ \vdots & \vdots & \cdots & \vdots & \vdots & \ddots & \vdots & \ddots & \vdots & \cdots & \ddots & \vdots & \vdots \\ 1-P_b & 0 & \cdots & 0 & 0 & \cdots & 0 & \cdots & 0 & \cdots & 0 & \cdots & P_b \\ \vdots & \vdots & \cdots & \vdots & \vdots & \ddots & \vdots & \ddots & \vdots & \ddots & \vdots & \ddots & \vdots \\ 0 & 0 & \cdots & 0 & 0 & \cdots & 0 & \cdots & 0 & \cdots & 0 & \cdots & P_b \\ 0 & 0 & \cdots & 0 & 0 & \cdots & 0 & \cdots & 0 & \cdots & 0 & \cdots & 1 \end{array} \right] \end{matrix} \quad (11)$$

$$\begin{aligned}
& P_{B_{c-1}} \\
& = P_{B_c} \mathbb{P}[B_c \rightarrow B_{c-1}] \\
& \stackrel{(a)}{=} \underbrace{\left[P_{ini}(c,k) + \underbrace{P_{B_{c+1}} \mathbb{P}[B_{c+1} \rightarrow B_c]}_{=P_{B_c}} \right]}_{\substack{\text{Directly from } B_0 \\ \text{Via } B_{c+1}}} \mathbb{P}[B_c \rightarrow B_{c-1}] \\
& \stackrel{(b)}{=} \left[P_{ini}(c,k) + \underbrace{\left\{ \underbrace{P_{ini}(c+1,k)}_{\text{Directly from } B_0} + \underbrace{P_{B_{c+2}} \mathbb{P}[B_{c+2} \rightarrow B_{c+1}]}_{\text{Via } B_{c+2}} \right\}}_{=P_{B_{c+1}}} \right] \mathbb{P}[B_{c+1} \rightarrow B_c] \mathbb{P}[B_c \rightarrow B_{c-1}] \\
& = \left[P_{ini}(c,k) + \left\{ P_{ini}(c+1,k) + \underbrace{\left(\underbrace{P_{ini}(c+2,k)}_{\text{Directly from } B_0} + \underbrace{P_{B_{c+2}} \mathbb{P}[B_{c+3} \rightarrow B_{c+2}]}_{\text{Via } B_{c+2}} \right)}_{=P_{B_{c+2}}} \right\} \mathbb{P}[B_{c+2} \rightarrow B_{c+1}] \right] \mathbb{P}[B_{c+1} \rightarrow B_c] \mathbb{P}[B_c \rightarrow B_{c-1}] \\
& \stackrel{(c)}{=} \left[P_{ini}(c,k) + \left\{ P_{ini}(c+1,k) + \underbrace{\left(\underbrace{P_{ini}(c+2,k)}_{\text{Directly from } B_0} + \underbrace{P_{B_{c+2}} (1-P_b)}_{\text{Via } B_{c+2}} \right)}_{=P_{B_{c+2}}} \right\} (1-P_b) \right] (1-P_b) \\
& \stackrel{(d)}{=} \text{The expansion is kept until reaching } \mathbb{P}[B_{CW-1}] \quad (12)
\end{aligned}$$

steady-state propagation for the Markov chain. Also, in (c), we substitute $\mathbb{P}[B_c \rightarrow B_{c-1}]$ with $1 - P_b$ as illustrated in Fig. 3. Lastly, (d) tells that the expansion shown in (12) goes until it reaches $\mathbb{P}[B_{CW-1}]$. It is important to note that state B_{CW-1} has only one input: directly from B_0 .

Now, the following two propositions present the formulation of a numerical solution for τ and P_b .

Proposition 6 (τ as a function of P_b). *The probability of reaching state B_0 is equivalent to the probability of a packet transmission after propagating through the Markov chain [23]. The general one-step steady-state transition shown in Proposition 5 can be applied to obtain the probability of transition from an arbitrary state B_c to P_{B_0} . In this paper, this transition formula provides a piece for the numerical solve of*

τ and P_b , which is given by

$$\begin{aligned}
\tau & := P_{B_0} \\
& = P_{B_1} \underbrace{(1 - P_b)}_{=P[B_1 \rightarrow B_0]} \\
& = \left(P_{ini}(1,k) + \underbrace{P_{B_2} (1 - P_b)}_{=P[B_2 \rightarrow B_1]} \right) (1 - P_b) \\
& = \left(P_{ini}(1,k) + (P_{ini}(2,k) + \cdots) (1 - P_b) \right) (1 - P_b). \quad (14)
\end{aligned}$$

Implication of (14) is that now tau is written as a function of P_b since all the $P_{ini}(c,k)$'s are known.

Proposition 7 (τ as a function of P_b and n_{cs}). *While the Markov chain describes a node's process of going through a backoff process in CSMA/CA, P_b is determined from the dynamics among the nodes competing for the channel. More specifically, all the nodes that are located in the carrier-sense*

range of the tagged vehicle become the competitors for the channel. The probability of a slot being found busy can be formulated as

$$\begin{aligned} P_b &= 1 - (1 - \tau)^{n_{cs}} \\ &\stackrel{(a)}{\approx} 1 - \left(1 - \frac{1}{2L_{bcn}}\right)^{\frac{1}{n_{cs}}} \end{aligned} \quad (15)$$

where n_{cs} denotes the number of nodes within a given node's range of carrier sensing. For (a), we remind the approximation described in Proposition 3.

Lemma 2 (Numerical solution for τ). We compute τ and P_b via numerical solve based on simultaneous equations composed of (14) and (15) that have been presented in Propositions 6 and 7, respectively. The simultaneous equations were to be solved via a sufficiently large number of iterations testing all the possible values for τ and P_b . However, the process of calculating τ has become easier thanks to the approximation shown in Proposition 3.

C. Probability of Transmission in a Certain Slot

Elaborating on τ found in the previous subsection, we derive the probability that an arbitrary node is able to transmit in the l th slot (where $l \in \{0, 1, \dots, L_{bcn} - 1\}$).

Lemma 3 (Probability of transmission in a certain slot). Let τ_l denote the probability that a node transmits in the l th slot within a beaconing period of L_{bcn} slots.

$$\tau_l = \begin{cases} \tau \sum_{m=0}^{l-1} \left[P_{\text{ini}}(m, k) \binom{l-1}{m} P_b^{(l-1)-m} (1 - P_b)^m \right], & 1 \leq l \leq \text{CW} \\ \tau \sum_{m=0}^{\text{CW}-1} \left[P_{\text{ini}}(m, k) \binom{l-1+q}{m} P_b^{(l-1)-m+q} (1 - P_b)^m \right], & \text{CW} < l \leq L_{bcn} - 1 \end{cases}$$

where $q = l - \text{CW}$, which is > 0 .

Proof: It is intuitive to start derivation of τ_l from breaking down as follows:

$$\begin{aligned} \tau_l &= \mathbb{P}[\text{Transmission in slot } l \\ &\quad | \text{Transmission within a beacon period}] \\ &\stackrel{(a)}{=} \tau \mathbb{P}[\text{Transmission in slot } l] \end{aligned} \quad (16)$$

where m gives the index of a slot within a beaconing period. Notice that in (a), independence is assumed between events of (i) a packet transmission in any slot within a beaconing period and (ii) the transmission occurring in a certain slot l .

Now, let us focus on the second term. It is significant to note that the very first slot (i.e., slot 0) within a beaconing period is spent for allocation of a backoff value itself. It yields that even if a node has been allocated the backoff of 0, the node transmits in the next slot (i.e., slot 1). If the node was

allocated the backoff of 1, the earliest slot in which the node can transmit is slot 2, which occurs when it experienced no busy slot. In case the node did have busy slots, it would be able to transmit in a slot later than slot 2. Therefore, the range of index l for the term $\mathbb{P}[\text{Transmission in slot } l]$ is given by $l \in \{1, 2, \dots, L_{bcn} - 1\}$. We proceed in the derivation as follows:

$$\begin{aligned} &\mathbb{P}[\text{Transmission in slot } l] \\ &\stackrel{(a)}{=} \begin{cases} \sum_{m=0}^{l-1} \mathbb{P}[\text{Transmission in slot } l \\ \quad | \text{Backoff} = m], & 1 \leq l \leq \text{CW} \\ \sum_{m=0}^{\text{CW}-1} \mathbb{P}[\text{Transmission in slot } l \\ \quad | \text{Backoff} = m], & \text{CW} < l \leq L_{bcn} - 1 \end{cases} \\ &\stackrel{(b)}{=} \begin{cases} \sum_{m=0}^{l-1} \left\{ P_{\text{ini}}(m, k) \right. \\ \quad \left. \mathbb{P}[\text{Transmission in slot } l] \right\}, & 1 \leq l \leq \text{CW} \\ \sum_{m=0}^{\text{CW}-1} \left\{ P_{\text{ini}}(m, k) \right. \\ \quad \left. \mathbb{P}[\text{Transmission in slot } l] \right\}, & \text{CW} < l \leq L_{bcn} - 1 \end{cases} \\ &\stackrel{(c)}{=} \begin{cases} \sum_{m=0}^{l-1} \left[P_{\text{ini}}(m, k) \binom{l-1}{m} P_b^{(l-1)-m} (1 - P_b)^m \right], & 1 \leq l \leq \text{CW} \\ \sum_{m=0}^{\text{CW}-1} \left[P_{\text{ini}}(m, k) \binom{l-1+q}{m} P_b^{(l-1)-m+q} (1 - P_b)^m \right], & \text{CW} < l \leq L_{bcn} - 1 \end{cases} \end{aligned}$$

where $q = l - \text{CW}$, which is > 0 .

In (a), the separation into two ranges of l is necessary because a transmission in a slot $\text{CW} < l \leq L_{bcn} - 1$ takes at least one busy slot regardless of the value of m . For instance, with $\text{CW} = 15$, a transmission in slot 16 given the greatest backoff value (i.e., $\text{CW} - 1 = 14$) is yielded from a busy slot. Note that the packet would have been transmitted in slot 15 if no busy slot was found.

In (b), $P_{\text{ini}}(m, k)$ denotes $\mathbb{P}[\text{Backoff} = m]$ where $k \in \{\text{decrease, flat}\}$ defines the pattern of backoff allocation as has described in Definition 3.

In (c), term $\mathbb{P}[\text{Transmission in slot } l]$ is modeled as binomial because as shown in Fig. 3, the probability is resulted from a combination of either P_b or $1 - P_b$. The number of P_b 's determines the number of backoff counter decrements; and the number of $(1 - P_b)$'s determines the number of slots spent while staying without being able to decrement the backoff counter.

Plugging (c) of $\mathbb{P}[\text{Transmission in slot } l]$ into (a) of τ_l completes the proof. \blacksquare

D. Packet Delivery Rate (PDR)

Appreciating its easiness to understand, this paper adopts the probability that a packet is successfully delivered to an arbitrary receiver vehicle (or PDR) as the key metric evaluating the proposed protocol in comparison to the original DSRC.

Lemma 4 (Probability of an EXP). *The probability that a node is not able to transmit in any slot within a beaconing period can be formulated as*

$$P_{\text{exp}} = 1 - \tau \quad (17)$$

Proof: It is significant to note that a backoff process of DSRC is “reset” after every beaconing period regardless of whether a packet is successfully transmitted or not. It means that the “steady-state” in DSRC is $t \approx L_{bcn} \times (\text{Slot time})$ rather than $t \rightarrow \infty$ as in other IEEE 802.11 standards. As such, cases of finishing at other states including B 's and D 's occur although a separate state of EXP exists in the backoff process model as shown in Fig. 3. Recall from Fig. 3 that state D_{c,δ_c} , the deepest state of a delay with backoff counter c , gives the last possible delay state before being drained to an EXP. It implies the possibility of staying at any other state than B_0 and EXP at the end of a beaconing period, which consequently should be added to the probability of an EXP. As a consequence, the probability of an EXP is obtained as $P_{\text{exp}} = 1 - \tau$. ■

Once a packet is transmitted, in order to lead to a successful delivery, no collision must occur on the packet during the transit. In other words, for a tagged vehicle, an external collision occurs unless both of the following conditions are satisfied: (1) when the tagged vehicle is transmitting, no vehicles within its carrier-sensing range delivery packets at the same time slot; and (2) when the tagged vehicle is transmitting, no hidden terminals should corrupt the tagged vehicle's packet.

To formulate, as just have mentioned, there are two types of collision in an IEEE 802.11-based network—namely, SYNC and HN [42]. Notice that the geometry for a SYNC is limited to the tagged vehicle's carrier-sense range because the packet collision occurs among the vehicles who are sensed but cannot avoid a collision due to allocation of a same backoff value [21]. On the other hand, the geometry for a HN is greater than a SYNC because the vehicles causing this type of packet collision are placed outside of the tagged vehicle's carrier-sense range [21], which figuratively defines “hidden nodes.”

Lemma 5 (Probability of a SYNC). *The probability that a packet collides over the air due to a synchronized collision is given by*

$$P_{\text{sync}} = \left\{ 1 - \left(1 - \frac{1}{2L_{bcn}} \right)^{n_{cs}} \right\} \left(1 - e^{-n_{cs}} \right) \frac{1}{L_{bcn}} \sum_{l=0}^{L_{bcn}-1} \tau_l \quad (18)$$

Proof: The formulation can be started from the following definition:

$$\begin{aligned} P_{\text{sync}} &= \mathbb{E}_l \left[\mathbb{P}[\text{SYNC in } l \mid \text{Transmission in slot } l \mid n_{cs} > 0] \right] \\ &= \sum_{l=0}^{L_{bcn}-1} \left[\mathbb{P}[\text{SYNC in } l] \mathbb{P}[\text{Transmission in slot } l] \right. \\ &\quad \left. \mathbb{P}[n_{cs} > 0] \mathbb{P}[l] \right] \quad (19) \end{aligned}$$

The first term is elaborated as

$$\begin{aligned} &\mathbb{P}[\text{SYNC in } l] \\ &= \mathbb{P}[\text{At least one other node transmits in slot } l] \\ &= 1 - \mathbb{P}[\text{No other node transmits in slot } l] \\ &\stackrel{(a)}{\approx} 1 - \left(1 - \frac{1}{2L_{bcn}} \right)^{n_{cs}}. \quad (20) \end{aligned}$$

Approximation (a) came from Proposition 3.

The second term of (19) indicates the probability of the tagged vehicle's transmission in slot l , which has already been found in Lemma 3 as $\mathbb{P}[\text{Transmission in slot } l] = \tau_l$.

The third term takes analysis on stochastic geometry. One critical condition for a point process to be a PPP is that the number of points falling in a bounded Borel set \mathcal{A} is a Poisson random variable with the parameter of $\lambda|\mathcal{A}|$, which is given by [61]

$$\mathbb{P}(\mathcal{A}) = \frac{(\lambda|\mathcal{A}|)^{n_{cs}} e^{-\lambda|\mathcal{A}|}}{n_{cs}!} \quad (21)$$

where $|\mathcal{A}|$ denotes the area of an arbitrary two-dimensional space \mathcal{A} . Refer to Figs. 6 and 7 of [21] that A_{col} forms a circular space in which a point x is located at the origin of the center and another point y is placed r away from the origin. That is, $|A_{\text{col}}| = \pi r_{cs}^2$. Based on this, we can exploit the CDF of the distance l between the two arbitrary points for calculation of $1 - \mathbb{P}(\text{No other node in } A_{\text{col}})$, which is written as

$$\begin{aligned} \mathbb{P}(n_{cs} > 0) &\stackrel{(a)}{=} \mathbb{P}(n > 0, A_{\text{col}}) \\ &= 1 - \mathbb{P}(n_{cs} = 0, A_{\text{col}}) \\ &= 1 - \frac{(\lambda\pi r_{cs}^2)^0 e^{-\lambda\pi r_{cs}^2}}{0!} \\ &= 1 - e^{-\lambda\pi r_{cs}^2}, \quad r_{cs} \geq 0. \quad (22) \end{aligned}$$

For (a), we assume the existence of two nodes at least: one for vT and the other as a potential SYNC-causing node.

The last term of (19) is given by $\mathbb{P}[l] = 1/L_{bcn}$. The rationale is that l is the index denoting each slot in a beaconing period, which yields that the significance of each slot is equal and uniform.

Therefore, the probability of a SYNC can be formulated as

$$\begin{aligned} P_{\text{sync}} &= \sum_{l=0}^{L_{bcn}-1} \left[\left\{ 1 - \left(1 - \frac{1}{2L_{bcn}} \right)^{n_{cs}} \right\} \tau_l \left(1 - e^{-\lambda\pi r_{cs}^2} \right) \frac{1}{L_{bcn}} \right] \\ &= \left\{ 1 - \left(1 - \frac{1}{2L_{bcn}} \right)^{n_{cs}} \right\} \left(1 - e^{-n_{cs}} \right) \frac{1}{L_{bcn}} \sum_{l=0}^{L_{bcn}-1} \tau_l \quad (23) \end{aligned}$$

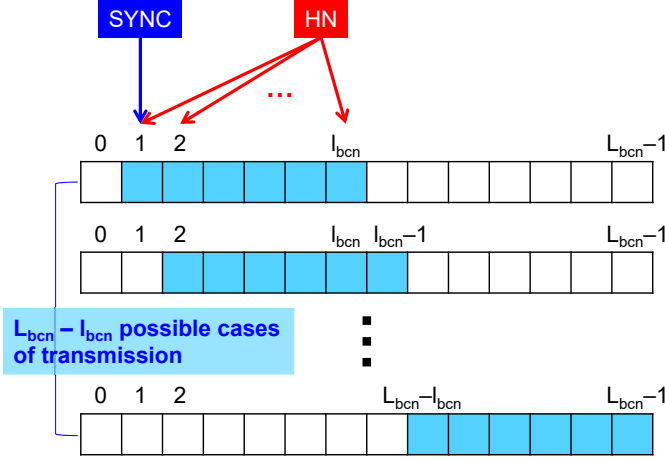


Fig. 6: All possible cases of a packet transmission within a beacon period

which completes the proof. ■

Lemma 6 (Probability of a HN). *The probability that a packet collides over the air due to a synchronized collision is given by*

$$P_{\text{hn}} = \left[1 - \left(1 - \frac{1}{2L_{\text{bcn}}} \right)^{n_{\text{hn}} l_{\text{bcn}}} \right] \left(1 - e^{-3\lambda\pi r_{cs}^2} \right) \frac{1}{L_{\text{bcn}} - l_{\text{bcn}}} \sum_{l=0}^{L_{\text{bcn}} - l_{\text{bcn}}} \tau_l \quad (24)$$

Proof: Before starting derivation of an equation, it is significant to note the critical difference between a SYNC and a HN. While a SYNC occurs in a single slot, a HN can occur at any time instant within an entire BSM (i.e., l_{bcn} slots). Specifically, there are two possible scenarios in which a hidden terminal fails a packet transmission of the tagged vehicle: (i) the tagged vehicle starts sending while a hidden terminal is transmitting, or (ii) a hidden terminal starts sending while the tagged vehicle is transmitting. As shown in Fig. 6, there are $L_{\text{bcn}} - l_{\text{bcn}}$ possible cases of BSM transmission. In each case, a BSM is highlighted in blue. Unlike a SYNC, any transmission by any hidden node causes HN collision.

Now, the formulation can be started from the following definition:

$$\begin{aligned} P_{\text{hn}} &= \mathbb{E}_l \left[\mathbb{P} \left[\text{HN in } l \mid \text{Transmission in slot } l \mid n_{cs} > 0 \right] \right] \\ &= \sum_{l=0}^{L_{\text{bcn}} - l_{\text{bcn}} - 1} \left[\mathbb{P} \left[\text{HN in } l \right] \cdot \mathbb{P} \left[\text{Transmission in slot } l \right] \mathbb{P} \left[n_{cs} > 0 \right] \mathbb{P} \left[l \right] \right] \quad (25) \end{aligned}$$

The first term of (25) can be elaborated as

$$\begin{aligned} \mathbb{P} \left[\text{HN in } l \right] &= \mathbb{P} \left[\text{At least one hidden node among } l_{\text{bcn}} \text{ slots} \right] \\ &= 1 - \mathbb{P} \left[\text{No hidden node among } l_{\text{bcn}} \text{ slots} \right] \\ &\stackrel{(a)}{\approx} 1 - \underbrace{\left(1 - \frac{1}{2L_{\text{bcn}}} \right)^{n_{\text{hn}}} \right)^{l_{\text{bcn}}}}_{\text{No HN in } l_{\text{bcn}} \text{ slots}} \\ &= 1 - \left(1 - \frac{1}{2L_{\text{bcn}}} \right)^{n_{\text{hn}} l_{\text{bcn}}} \quad (26) \end{aligned}$$

In (a), the approximation came from Proposition 3. Also, as has already been mentioned, a packet corruption by a hidden node does not need to occur in the same time slot with the starting slot of the tagged vehicle. As such, for no HN, none of the l_{bcn} slots should experience a HN.

Same with SYNC, the second term denotes the probability that the tagged vehicle transmits in slot l , which can also be found as $\mathbb{P} \left[\text{Transmission in slot } l \right] = \tau_l$.

The third term can be formulated, recalling from (22) but reflecting the larger area of potential HN-causing nodes being placed, which is given by [21]

$$\mathbb{P} \left[n_{cs} > 0 \right] = 1 - e^{-3\lambda\pi r_{cs}^2} \quad (27)$$

where the area of a HN has been found as a donut-shaped region formed between circumferences with the radii of r_{cs} and $2r_{cs}$ as illustrated in Fig. 17 of [21].

The last term of (25) denotes the significance of each slot l among all the possible cases where the tagged vehicle is able to transmit. It is given by $\mathbb{P} \left[l \right] = 1 / (L_{\text{bcn}} - l_{\text{bcn}})$, considering that the significance of each slot is equal and uniform.

Therefore, the probability of a HN can be formulated as

$$\begin{aligned} P_{\text{hn}} &= \sum_{l=0}^{L_{\text{bcn}} - l_{\text{bcn}}} \left[\left[1 - \left(1 - \frac{1}{2L_{\text{bcn}}} \right)^{n_{\text{hn}} l_{\text{bcn}}} \right] \tau_l \right. \\ &\quad \left. \left(1 - e^{-3\lambda\pi r_{cs}^2} \right) \frac{1}{L_{\text{bcn}} - l_{\text{bcn}}} \right] \\ &= \left[1 - \left(1 - \frac{1}{2L_{\text{bcn}}} \right)^{n_{\text{hn}} l_{\text{bcn}}} \right] \left(1 - e^{-3\lambda\pi r_{cs}^2} \right) \frac{1}{L_{\text{bcn}} - l_{\text{bcn}}} \sum_{l=0}^{L_{\text{bcn}} - l_{\text{bcn}}} \tau_l, \quad (28) \end{aligned}$$

which completes the proof. ■

Theorem 1 Based on the parameters defined through this paper, the PDR is formulated as

$$\text{PDR} = \tau \left(1 - P_{\text{sync}} \right) \left(1 - P_{\text{hn}} \right) \quad (29)$$

where P_{sync} and P_{hn} indicate the probabilities of a collision due to synchronized transmission and a hidden node.



Fig. 7: Formulation of IRT as a geometric distribution

Proof:

$$\begin{aligned}
 & \text{PDR} \\
 &= \mathbb{P}[\text{No collision over the air} \mid \text{Packet transmission}] \\
 &\stackrel{(a)}{=} \underbrace{\tau (1 - P_{\text{sync}}) (1 - P_{\text{hn}})}_{=\mathbb{P}[\text{No collision over the air}]} \quad (30)
 \end{aligned}$$

(a) follows from the assumption that the two events, “No collision over the air” and “Packet transmission,” are independent.

■

Remark 5 As shall be elaborated in Section VI-C, values of P_{sync} and P_{hn} are very small, which stay at the levels of 10^{-4} as demonstrated in Figs. 11 and 12. In accordance to it, PDR can be approximated as

$$\text{PDR} = \tau (1 - P_{\text{sync}}) (1 - P_{\text{hn}}) \approx \tau. \quad (31)$$

E. IRT

The second metric through which the performance of the proposed protocol is evaluated is the IRT. Fig. 7 illustrates the formulation of an IRT as a geometric distribution.

Notice that the unit of a quantity of IRT is “the number of slots.” As such, one needs to multiply a slot time when needing to display an IRT in the unit of time (i.e., seconds).

Lemma 7 (Distribution of IRT). *As aforementioned, the probability that an IRT occurs in the next k th beaconing period after the last successful delivery follows a geometric distribution, which can be formally written as*

$$\text{IRT} = (1 - \text{PDR})^{\nu-1} \text{PDR} \quad (32)$$

where ν denotes the number of unsuccessful receptions.

Proof: For occurrence of an “IRT,” we suppose to start from a successful reception, then measure how many beaconing periods are needed until the next successful reception. This is the reason that in Fig. 7, the first beaconing period is set to have the probability of PDR, and thereafter the possibility is left open between PDR and $1 - \text{PDR}$. It is formally written as

$$\begin{aligned}
 \text{IRT} &\sim \text{Geo}(\text{PDR}) \\
 &= \mathbb{P}[\text{IRT} = \nu] \\
 &= (1 - \text{PDR})^{\nu-1} \text{PDR} \quad (33)
 \end{aligned}$$

■

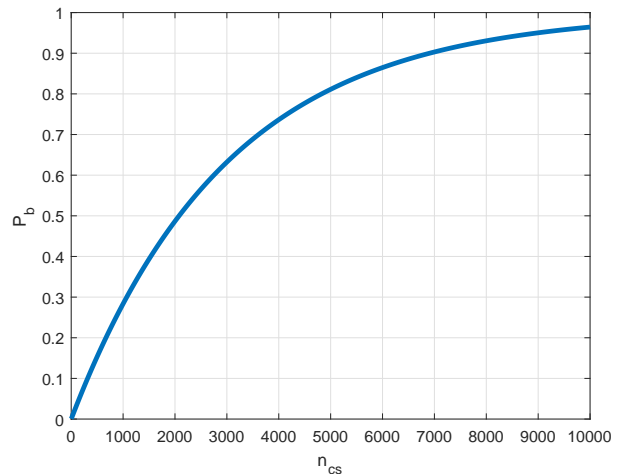


Fig. 8: P_b versus n_{cs}

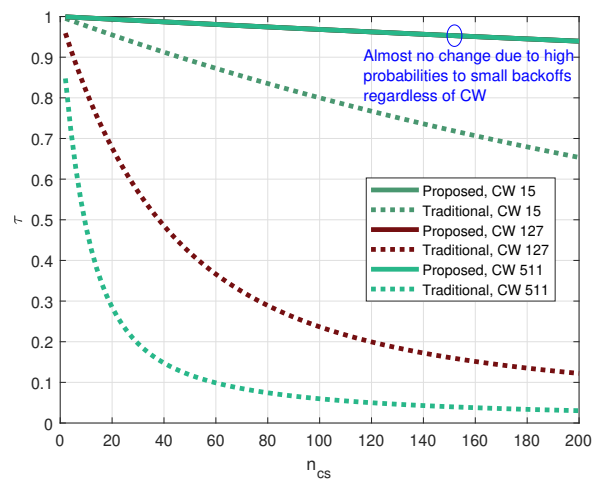


Fig. 9: τ versus n_{cs}

VI. RESULTS AND DISCUSSIONS

This section verifies the accuracy of the analysis presented in Section V, by comparing to Monte Carlo simulations of the network defined in Section III.

A. P_b

Fig. 8 demonstrates the P_b that has been resulted from the “uniform” approximated τ . Overall, the probability that a certain slot is found busy with another node can be kept relatively low—i.e., around 15% even with 500 competing nodes within one’s carrier-sense range. The reason is the small value for τ as shown in Fig. 9, which is plausible because a beaconing period contains a very large number of slots—i.e., L_{bcn} is as large as 1,500 with 100 msec and $66.7 \mu\text{sec}$ for a beaconing period and a slot time, respectively.

Also, the results match one’s intuitions: P_b is increased with a greater n_{cs} . One can observe that a smaller value of r yields a lower P_b (which, in turn, leads to a higher P_{start} as such). The rationale behind this result is that a smaller r serves as a more drastic decrement of P_{ini} as shown in (8).

■

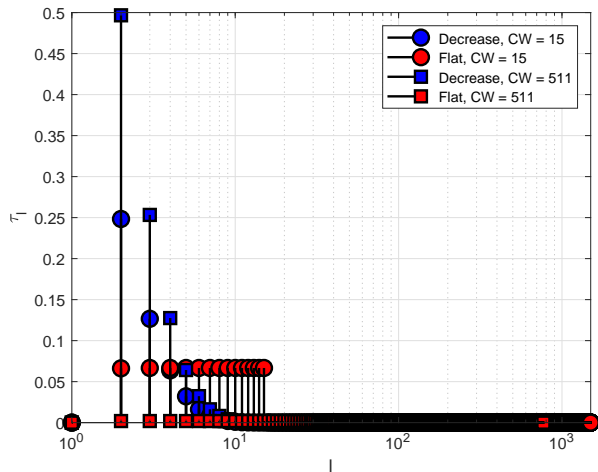


Fig. 10: τ_l for each l within a beaoning period (CW = 15 and $n_{cs} = 20$)

B. τ and τ_l

Fig. 9 shows the probability that a vehicle has been able to go through a backoff process and transmit a BSM, denoted by τ , versus the number of vehicles within its carrier-sense range. Notice that the key change from the reference [21] is the Markov chain due to proposition of P_{ini} .

Fig. 10 demonstrates the probability that a vehicle transmits a BSM within an arbitrary slot l , denoted by τ_l , for each slot l within a beaoning period when CW = 15. According to the difference in backoff allocation pattern (which has been shown in Definition 3), the proposed scheme (blue circle) shows higher probabilities of transmitting in earlier slots within a beaoning period compared to the traditional CSMA/CA (red square).

C. P_{hn} and P_{sync}

Figs. 11 and 12 demonstrate the probabilities of collision by a SYNC and HN, respectively. The probabilities are presented versus n_{cs} according to the backoff function type and CW. There are several important points to discuss from Figs. 11 and 12.

- The first and most striking one is that P_{hn} and P_{sync} are very small to the scale of 10^4 . The rationale is that there are a very large number of slots (i.e., $L_{bcn} = 1500$) within a beaoning period and thus the probability of a slot being found busy has been approximated to be very small (i.e., $1/2L_{bcn}$) as has been discussed in Fig. 5. This implies that DSRC has already been designed to robust against channel competition up to quite a large amount of traffic.
- Second, there is not much change in P_{hn} and P_{sync} with different CW's. The reasoning is that τ_l is a function of CW but less dominant than $1/L_{bcn}$ and $1/(L_{bcn} - l_{bcn})$ for SYNC and HN, respectively.
- Third, the probabilities do not make much difference between the decreasing and flat types of backoff function for the same reason.

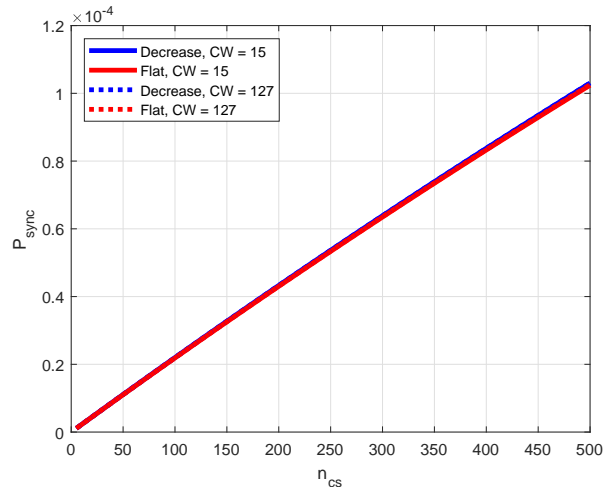


Fig. 11: P_{sync} versus n_{cs}

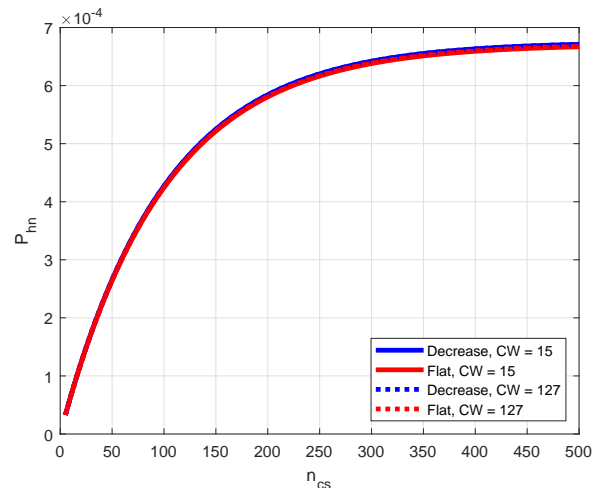


Fig. 12: P_{hn} versus n_{cs}

The aforementioned observation and discussions lead to a very significant remark:

Remark 6 (Dominance of performance by contention). *As observed from Figs. 9 and 11-12, it is evident that a PDR is dominated by τ rather than P_{sync} and P_{hn} . It implies that the successful delivery of a BSM is more about whether a node is able to start a transmission, rather than a transmitted packet collides with another over the air. In other words, it is interpreted that in DSRC, once a packet is transmitted, it will likely be delivered.*

Lemma 8 (Approximation of PDR). *Therefore, for values of PDR, one can refer to Fig. 9. As already discussed, due to very small values of P_{sync} and P_{hn} over a wide range of n_{cs} , a PDR can be approximated to be equivalent to τ .*

Proof: Remark 6 can be considered as a proof. ■

D. IRT

Fig. 13 shows the probability mass function (PMF) of IRT with respect to the number of slots until the next successful

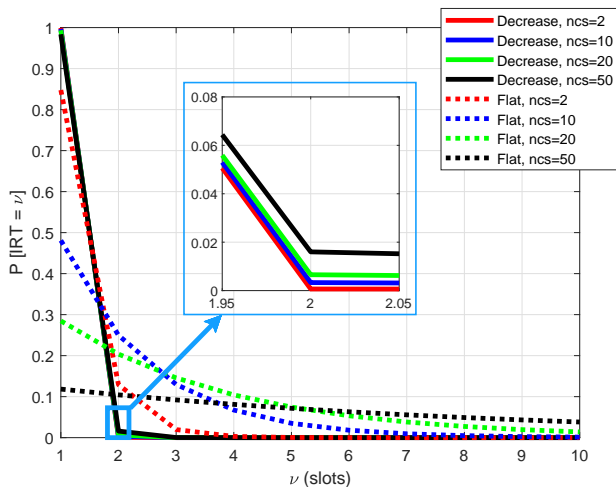


Fig. 13: IRT versus ν

packet delivery, ν . Notice that the IRT is written in terms of the number of slots, which can be straightforwardly converted to a time length by multiplying a slot time. For instance, with a slot time being $66.7 \mu\text{sec}$ [42], $\text{IRT} = 2$ in Fig. 13 can be interpreted to $133.4 \mu\text{sec}$ of latency between two consecutive packets.

One can observe that almost all packets can be delivered in the next slot for the dangerous vehicles who are allocated the backoff times in the decreasing pattern. Also, such priority remains unchanged even if the medium is competed among a larger number of users, which is attributed to τ (and approximately PDR) remaining not much impacted due to increase in n_{cs} as shown in Fig. 9.

Meanwhile, the IRT for nodes at normal speed variance Ψ (which hence is allocated flat backoff pattern) is influenced significantly by the number of competing nodes. Specifically, as the number of nodes grows, $\mathbb{P}[\text{IRT} = 1]$ gets suppressed down and $\mathbb{P}[\text{IRT} > 1]$ takes the spread.

VII. CONCLUSIONS

This paper proposed a backoff allocation scheme that is adaptive to the level of accident risk to which a vehicle is exposed. The proposed scheme requires a minimal modification of the current CSMA mechanism adopted for IEEE 802.11p, which can achieve higher generality and applicability to practice. We first identified the driving speed as a key factor determining a crash risk. For analysis, we defined the variance of speed as the key metric and presented closed-form expressions for the probability distribution of the metric. Then, we modeled the IEEE 802.11p CSMA as a Markov process, from which further performance evaluation metrics were derived: i.e., probabilities of transmission within a beaconing period, transmission within a certain slot, collision by a SYNC, collision by a HN, and IRT. From the analysis and numerical results, the main finding was that the performance of a BSM broadcast in an IEEE 802.11p network is predominated by contention rather than collision.

As such, this work has many possible extensions. The key merit of this work is identification of a factor that is critical

in causing an accident among the ones that can be obtained on a vehicle autonomously without any external support from infrastructure (e.g., RSU), which fits the “distributed” nature of a V2X network. One possible extension is to examine the feasibility of the proposed mechanism for a completely distributed consensus algorithm (e.g., practical Byzantine fault tolerance) for blockchain. Considering that the decentralization is being regarded as one of the most critical factors in the blockchain, the complete decentralization achieved by the proposed scheme will form a critical basis for establishing analytical frameworks for such blockchain-related extension.

REFERENCES

- [1] US FCC, *Dedicated short range communications (DSRC) service*, Apr. 2019. [Online]. Available: <https://www.fcc.gov/wireless/bureau-divisions/mobility-division/dedicated-short-range-communications-dsrc-service>
- [2] US FCC, *The commission seeks to update and refresh the record in the “unlicensed national information infrastructure (U-NII) devices in the 5 GHz band” Proceeding*, FCC 16-68A1.
- [3] 5GAA, “The case for cellular V2X for safety and cooperative driving,” Nov. 2016. [Online]. Available: <http://5gaa.org/wp-content/uploads/2017/10/5GAA-whitepaper-23-Nov-2016.pdf>
- [4] K. Bode, “5G could actually make the ‘digital divide’ worse,” *Techdirt Wireless*, Feb. 2020. [Online]. Available: <https://www.techdirt.com/articles/20200204/07071543850/5g-could-actually-make-digital-divide-worse.shtml>
- [5] J. Van Roy, “EU parliament finally votes for wifi to connect cars,” *New Mobility News*, Apr. 2019. [Online]. Available: <https://newmobility.news/2019/04/18/eu-parliament-finally-votes-for-wifi-to-connect-cars/>.
- [6] AASHTO, “State DOTs sign letter supporting preservation of 5.9 GHz spectrum,” *AASHTO J.*, Aug. 2019. [Online]. Available: <https://aashtojournal.org/2019/08/23/state-dots-sign-letter-supporting-preservation-of-5-9-ghz-spectrum/>.
- [7] US FCC, “Phase I testing of prototype U-NII-4 devices,” *TR 17-1006*, Oct. 2018.
- [8] AASHTO, *Re: Docket No. DOT-OST-2018-0210*, Feb. 2019. [Online]. Available: <https://policy.transportation.org/wp-content/uploads/sites/59/2019/02/AASHTO-Comments-USDOT-V2X-Communication-RFC-FINAL.pdf>
- [9] A. Weinfeld, “Methods to reduce DSRC channel congestion and improve V2V communication reliability,” in *Proc. ITS World Congress 2010*.
- [10] US FCC, “In the matter of use of the 5.850-5.925 GHz band,” *Notice of Proposed Rulemaking*, ET Docket No. 19-138, FCC 19-129, Dec. 2019.
- [11] S. Kim, J. Park, and K. Bian, “PSUN: An OFDM transmission strategy for coexistence with pulsed radar,” in *Proc. IEEE ICNC 2015*.
- [12] S. Kim, J. Choi, and C. Dietrich, “PSUN: an OFDM - pulsed radar coexistence technique with application to 3.5 GHz LTE,” *Hindawi Mobile Inform. Syst. J.*, Jul. 2016.
- [13] S. Kim, J. Choi, and C. Dietrich, “Coexistence between OFDM and pulsed radars in the 3.5 GHz band with imperfect sensing,” in *Proc. IEEE WCNC 2016*.
- [14] S. Kim and C. Dietrich, “Coexistence of outdoor Wi-Fi and radar at 3.5 GHz,” *IEEE Wireless Commun. Lett.*, vol. 6, iss. 4, Aug. 2017.
- [15] S. Kim, E. Visotsky, P. Moorut, K. Bechta, A. Ghosh, and C. Dietrich, “Coexistence of 5G with the incumbents in the 28 and 70 GHz bands,” *IEEE J. Sel. Areas Commun.*, vol. 35, iss. 8, Aug. 2017.
- [16] M. Kabir and S. Kim, “5G or Wi-Fi for HA/DR in the 60 GHz Band?,” in *Proc. IEEE Int. Symp. Technol. Homeland Security 2019*.
- [17] J. Verboom and S. Kim, “Stochastic analysis on downlink performance of coexistence between WiGig and NR-U in 60 GHz band,” *arXiv:2003.01570*, Mar. 2020.
- [18] S. Kim and T. Dessalgn, “Mitigation of civilian-to-military interference in DSRC for urban operations,” in *Proc. IEEE MILCOM 2019*.
- [19] S. Kim and B. J. Kim, “Prioritization of basic safety message in DSRC based on distance to danger,” *arXiv:2003.09724*, Mar. 2020.

- [20] J. W. Tantra, C. H. Foh, and A. Ben Mnaouer, "Throughput and delay analysis of the IEEE 802.11e EDCA saturation," in *Proc. IEEE ICC 2005*.
- [21] S. Kim and M. Bennis, "Spatiotemporal analysis on broadcast performance of DSRC with external interference in 5.9 GHz band," *arXiv:1912.02537*, Dec. 2019. [Online]. Available: <https://arxiv.org/pdf/1912.02537.pdf>
- [22] S. Kim, "Impacts of mobility on performance of blockchain in VANET," *IEEE Access*, vol. 7, May 2019.
- [23] G. Bianchi, "IEEE 802.11-saturation throughput analysis," *IEEE Commun. Lett.*, vol. 12, no. 2, Dec. 1998.
- [24] X. Yin, X. Ma, and K. S. Trivedi, "An interacting stochastic models approach for the performance evaluation of DSRC vehicular safety communication," *IEEE Trans. Comput.*, vol. 62, no. 5, May 2013.
- [25] IEEE 802.11p Standard, "802.11p-2010 - IEEE Standard for Information technology- Local and metropolitan area networks- Specific requirements- Part 11: Wireless LAN Medium Access Control (MAC) and Physical Layer (PHY) Specifications Amendment 6: Wireless Access in Vehicular Environments," Jun. 2010.
- [26] IEEE 802.11 Standard, "802.11-2016 - IEEE Standard for Information technology-Telecommunications and information exchange between systems Local and metropolitan area networks-Specific requirements - Part 11: Wireless LAN Medium Access Control (MAC) and Physical Layer (PHY) Specifications," Dec. 2016.
- [27] Y. Yao, L. Rao, X. Liu, "Performance and reliability analysis of IEEE 802.11p safety communication in a highway environment," *IEEE Trans. Veh. Technol.*, vol. 62, no. 9, 2013.
- [28] M. Khabazian, S. Aissa, M. Mehmet-Ali, "Performance modeling of safety messages broadcast in vehicular ad hoc networks," *IEEE Trans. Intell. Transp. Syst.*, vol. 14, no. 1, 2013.
- [29] X. Lei and S. H. Rhee, "Performance analysis and enhancement of IEEE 802.11p beaconing," *EURASIP J. Wireless Commun. Netw.*, vol. 2019, no. 61, Dec. 2019.
- [30] S. Son and K.-J. Park, "BEAT: beacon inter-reception time ensured adaptive transmission for vehicle-to-vehicle safety communication," *MDPI Sensors*, vol. 19, no. 14, Jul. 2019.
- [31] T. ElBatt, S. K. Goel, G. Holland, H. Krishnan, and J. Parikh, "Cooperative collision warning using dedicated short range wireless communications," in *Proc. ACM VANET 2006*.
- [32] G. Jornod, A. El Assaad, A. Kwoczek, and T. Kurner, "Packet inter-reception time modeling for high-density platooning in varying surrounding traffic density," in *Proc. IEEE EuCNC 2019*.
- [33] T. T. Almeida, L. de C. Gomes, F. M. Ortiz, J. G. R. Junior, and L. H. M. K. Costa, "IEEE 802.11p performance evaluation: simulations vs. real experiments," in *Proc. IEEE ISTC 2018*.
- [34] B. Cheng, H. Lu, A. Rostami, M. Gruteser, and J. B. Kenney, "Impact of 5.9 GHz spectrum sharing on DSRC performance," in *Proc. IEEE VNC 2017*.
- [35] I. Khan, G. M. Hoang, and J. Harri, "Rethinking cooperative awareness for future V2X safety-critical applications," in *Proc. IEEE VNC 2017*.
- [36] Z. Liu, Z. Liu, Z. Meng, X. Yang, L. Pu, and L. Zhang, "Implementation and performance measurement of a V2X communication system for vehicle and pedestrian safety," *Internat. J. Distributed Sensor Netw.*, vol. 12, no. 9, Sep. 2016.
- [37] M. E. Rendaa, G. Restaa, P. Santi, F. Martelli, and A. Franchini, "IEEE 802.11p VANets: experimental evaluation of packet inter-reception time," *Elsevier Comput. Commun.*, vol. 75, Feb. 2016.
- [38] M. Torrent-Moreno, J. Mittag, P. Santi, and H. Hartenstein, "Vehicle-to-vehicle communication: Fair transmit power control for safety-critical information," *IEEE Trans. Veh. Technol.*, vol. 58, no. 7, Mar. 2009.
- [39] B. Kloiber, J. Harri, T. Strang, S. Sand, and C. R. Garcia, "Random transmit power control for DSRC and its application to cooperative safety," *IEEE Trans. Dependable Secur. Comput.*, vol. 13, no. 1, Jun. 2015.
- [40] C. L. Huang, Y. P. Fallah, R. Sengupta, and H. Krishnan, "Intervehicle transmission rate control for cooperative active safety system," *IEEE Trans. Intell. Transp. Syst.*, vol. 12, no. 3, Oct. 2010.
- [41] Y. P. Fallah, C. L. Huang, R. Sengupta, and H. Krishnan, "Analysis of information dissemination in vehicular ad-hoc networks with application to cooperative vehicle safety systems," *IEEE Trans. Veh. Technol.*, vol. 60, no. 1, Oct. 2010.
- [42] R. Stanica, E. Chaput, and A.-L. Beylot, "Reverse back-off mechanism for safety vehicular ad hoc networks," *Elsevier Ad Hoc Networks*, vol. 16, May 2014.
- [43] C. Song, "Performance analysis of the IEEE 802.11p multichannel MAC protocol in vehicular ad hoc networks," *MDPI Sensors*, vol. 17, 2017.
- [44] A. I. Abu-Khadrah, A. Zakaria, M. Othman, and M. S. Zin, "Enhance the performance of EDCA protocol by adapting contention window," *Springer Wireless Personal Communications*, vol. 96, no. 2, Sep. 2017.
- [45] R. Moraes, P. Portugal, F. Vasques, and R. F. Custodio, "Assessment of the IEEE 802.11e EDCA protocol limitations when dealing with real-time communication," *EURASIP J. Wirelss Commun. Netw.*, Dec. 2010.
- [46] S. Kim and Y. J. Cho, "Adaptive transmission opportunity scheme based on delay bound and network load in IEEE 802.11e wireless LANs," *J. Appl. Res. Technol.*, vol. 11, no. 4, Aug. 2013.
- [47] P. Patel and D. K. Lobiyal, "A simple but effective collision and error aware adaptive back-off mechanism to improve the performance of IEEE 802.11 DCF in error-prone environment," *Springer Wireless Pers. Commun.*, vol. 83, no. 2, Jul. 2015.
- [48] M. Karaca, S. Bastani, and B. Landfeldt, "Modifying backoff freezing mechanism to optimize dense IEEE 802.11 networks," *IEEE Trans. Veh. Technol.*, vol. 66, no. 10, Oct. 2017.
- [49] M. AlHubaishi, T. Alahdal, R. Alsaqour, A. Berqia, M. Abdelhaq, and O. Alsaqour, "Enhanced binary exponential backoff algorithm for fair channel access in the IEEE 802.11 medium access control protocol," *Int. J. Commun. Syst.*, vol. 27, no. 12, Dec. 2014.
- [50] N. O. Song, B. J. Kwak, J. Song, and M. Miller, "Enhancement of IEEE 802.11 distributed coordination function with exponential increase exponential decrease backoff algorithm," in *Proc. IEEE VTC 2003-Spring*.
- [51] K. Ashrafuzzaman and A. O. Fapojuwo, "Efficient and agile CSMA in capillary M2M communication networks," *IEEE Access*, vol. 6, Jan. 2018.
- [52] S. Kim, "Coexistence of wireless systems for spectrum sharing," *PhD Dissertation*, Virginia Tech, Jul. 2017.
- [53] T. Dessalgn and S. Kim, "Danger aware vehicular networking," in *Proc. IEEE SoutheastCon 2019*.
- [54] S. Kim and B. J. Kim, "Reinforcement learning for accident risk-adaptive V2X networking," *arXiv:2004.02379*, Apr. 2020.
- [55] S. Kim and C. Dietrich, "A novel method for evaluation of coexistence between DSRC and Wi-Fi at 5.9 GHz," in *Proc. IEEE Globecom 2018*.
- [56] D. Daley and D. Vere-Jones, *An Introduction to the Theory of Point Processes: Volume I: Elementary Theory and Methods*, Springer Probability and its Applications, Second edition, 2003.
- [57] S. N. Chiu, D. Stoyan, W. S. Kendall, and J. Mecke, *Stochastic Geometry and Its Applications*, pp. 3840 and 5354, Jun. 2013.
- [58] US Department of Transportation, "Speed concepts: informational guide," *Publication No. FHWA-SA-10-001*, pp. 17-19, Sep. 2009.
- [59] W. Manda, S. H. Steiner, R. J. MacKay, and A. R. Hilal, "Using telematics data to find risky driver behaviour," *Accident Analysis & Prevention*, Aug. 2019. [Online]. Available: <https://www.sciencedaily.com/releases/2019/08/190821082233.htm>
- [60] G. Bianchi, "Performance analysis of the IEEE 802.11 distributed coordination function," *IEEE J. Sel. Areas Commun.*, vol. 18, no. 3, Mar. 2000.
- [61] M. Haenggi, "On distances in uniformly random networks," *IEEE Trans. Inf. Theory*, vol. 51, no. 10, Oct. 2005.